Analysis of an Arc Light Mechanism and Its Application in Sensing of the GTAW Process

A theoretical model was developed that correlates arc light radiation with welding parameters

BY P. J. LI AND Y. M. ZHANG

ABSTRACT. Sensing plays a key role in automating and controlling welding processes. In recent decades, arc light sensing has been studied for arc length control, joint tracking and droplet transfer detection in arc welding. However, the current technology relies on experimental data and lacks theoretical foundation. To improve measurement accuracy, this work addresses the theoretical foundation for arc light sensing. A theoretical model has been developed to correlate arc light radiation to welding parameters. Distributions of different radiant sources in the arc column are studied. It is found that the distributions of the ions of the shielding gas and the vapors of the base metal and tungsten are not even, while that of the shielding gas atoms is. This suggests the spectral lines associated with the shielding gas atoms can be used to improve the accuracy of arc light sensing. Hence, an arc light sensor has been developed to detect argon atom spectral lines in gas tungsten arc welding. The relationship between the argon lines and the welding parameters has been derived from the theoretical model. Joint tracking examples showed the effectiveness of the developed method in improving accuracy.

Introduction

Arc light radiation is a fundamental phenomenon associated with the arc welding process. Early studies were primarily dedicated to investigating its hazardous effects (Refs. 1–6). Topics included harm to human beings, correlation between welding process and arc light intensity, as well as the relationship between hazardous effects and the spectral bands of the arc light. Commercial welding curtains and shades resulted from these studies (Ref. 7).

Arc light is closely related to the plasma column of the arc. By means of spectral analysis of arc light, temperature distribution and conductivity of the arc column (Refs. 8–16), temperature and emissivity of tungsten (Refs. 17–20), droplet temperature (Refs. 21, 22), hydrogen density in the arc column (Refs. 23, 24) and temperature of the weld pool surface (Refs. 25–28) were measured and analyzed. The spectral analysis method has also been used to study the influence of minor elements on weldability (Refs. 29–31).

Early utilization of arc light in process sensing was based on its optical property. In the work by Faber and Jackel, two symmetrically arranged, light-sensitive components were used to achieve joint tracking in fillet welding by compensating their difference in the incident light intensity (Ref. 32). Nomura used four CdS components implanted in a water-cooled copper plate placed at the backside of the weld pass to monitor the keyhole (Refs. 33, 34). In research by Deam and Connelly, vibration frequency of the weld pool in gas tungsten arc welding (GTAW) was monitored by sensing the arc light reflected by the mirror-like surface of the weld pool (Refs. 35–37).

A few further studies investigated the possibility of sensing welding behaviors based on arc light. In particular, a U.S. patent (Ref. 38) introduced a method for arc length sensing in which the integral intensity of arc light in the ultraviolet band was monitored to improve its sensing accuracy. In another research work, an arc light sensor was used to monitor the droplet transfer mode in GMAW (Refs. 39, 40). The sensitivity of arc light sensing in this application is higher than that of arc electric signal sensing and arc sound sensing (Refs. 41–44).

Extensive efforts were made by Richardson and Edwards (Ref. 45) toward revealing the feasibility of arc light sensing, such as investigating the sensitivity and stability of arc light in comparison with the prevalent sensing method — arc voltage sensing — in arc length measurement. Their work showed arc light sensing has better accuracy and stability, and the authors also explained the advantage of this sensing method.

Although encouraging progress was obtained based on these works, the application of arc light sensing is still limited. Arc light radiation is a complicated phenomenon involving several welding parameters. Without understanding the essential mechanism, its utilization is based on merely subjective experience and assumptions. To guide the applica-

P. J. LI and Y. M. ZHANG are with the Welding Research Laboratory, Center for Robotics and Manufacturing Systems and Electrical Engineering Department, College of Engineering, University of Kentucky, Lexington, Ky.

KEY WORDS

Arc Light
Sensing
Spectral Analysis
GTAW
Joint Tracking
Plasma Column
Sensor Accuracy

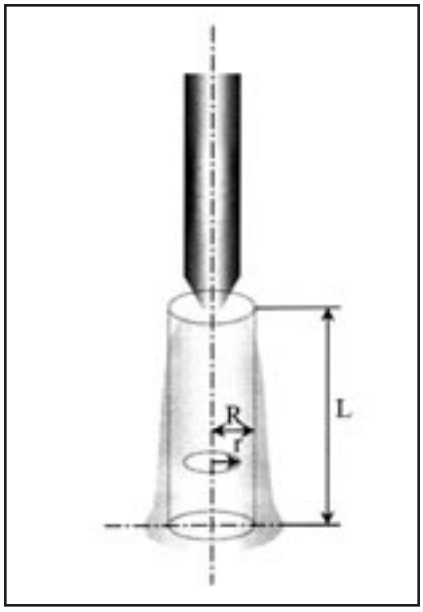

Fig. 1 — A model of the luminary of welding arc plasma.

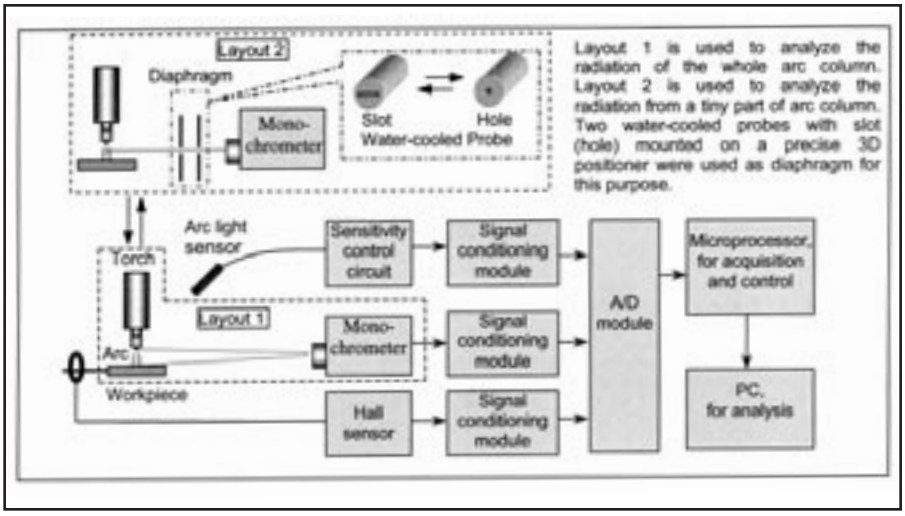

Fig. 2 — Experimental setup of the arc light radiation study.

tion of arc light sensing and to achieve high accuracy and reliability, the mechanism must be known. Hence, this paper is dedicated to establishing an arc light radiation model to correlate the arc light with the welding parameters. The dominant elements and their roles in determining the radiation are analyzed. The most sensitive spectra of the arc light, with respect to different welding behaviors, were analyzed and separated to improve the signal quality.

Model of Arc Light Sensing

During arc welding, the shielding gas in the plasma column can be assumed to consist of three kinds of particles: electrons, ions and excited neutral atoms. The plasma column can be assumed to be approximately in the local thermodynamic equilibrium (LTE) condition (Refs. 46, 47) in which electron collision plays an important role in excitation and ionization. The emission of arc light from a plasma is characterized by the emission coefficient ε_ν. According to Planck's Radiation Law and Kirchhoff's Law (Refs. 48, 49), it can be expressed as

$$\varepsilon_\nu = k'(\nu)\cdot B_\nu = k'(\nu)\cdot\frac{2\cdot h\cdot \nu^3}{c^2\cdot\left(e^{\frac{h\cdot\nu}{k\cdot T_e}}-1\right)} \quad (1)$$

where B_ν is the radiant energy, which is emitted by a unit volume of the radiating gas per unit of time, per unit of solid angle and per unit of wavelength; $k'(\nu)$ is a frequency-dependent absorption coefficient; c is velocity of light (2.9979 x 10^8 m·s^{-1}); T_e is electron temperature in K; ν is spectral frequency in Hz; k is Boltzmann's constant (1.3807 x 10^{-23} J·K^{-1}); and h is Planck's constant (6.6262 x 10^{-34} J·s).

Equation 1 describes the continuous emission of arc light radiation. Line emission is another fraction of the total light radiation from the arc (probably 15–20% of the total). Line emission follows roughly equivalent mathematics. Therefore, Equation 1 can be used for simplifying the derivation of the arc radiation model without introducing significant error.

When $h\nu/kT<<1$, the Rayleigh-Jeans radiation law holds (Refs. 48, 49). Thus, Equation 1 can be simplified as

$$\varepsilon_\nu \approx k'(\nu)\cdot 2\frac{\nu^2}{c^2}kT_e \quad (2)$$

The agreement of Equation 2 with 1 is better than 5% for $\lambda_L T > 4.3$ cm·K; λ_L is wavelength in cm (Ref. 48). According to research by Olsen, Kobayashi and Suga (Refs. 50, 51), the arc temperature in the gas tungsten welding process is more than 10,000 K. Thus, Equation 2 is equal to 1 approximately for the infrared band and most of the visible band of arc radiation. Also, under the atmospheric pressure and normal welding current range, the temperature of the electrons is very close to that of the arc (Ref. 52). Compared with the temperature of the arc, the difference is negligible. As a result,

$$\varepsilon_\nu = k'(\nu)\cdot 2\frac{\nu^2}{c^2}kT \quad (3)$$

where T is the temperature of the arc in K.

Assume that heat losses are all due to conduction (Ref. 49), then the Elenbass-Heller rule (Ref. 46) holds for any unit component in the arc column

$$\sigma\cdot E^2 + \frac{1}{r}d\left(\frac{r\lambda dT}{dr}\right)/dr = 0 \quad (4)$$

where E is voltage gradient of arc; r is distance of the unit component to axis of arc column, m; λ is thermal conductivity, W·m^{-1}·K^{-1}; and σ is electric conductivity.

In the welding arc column, electric conductivity will decrease to zero abruptly beyond a certain radius R (Ref. 53). It can be assumed approximately that welding current is constant within a column of R in radius, as shown in Fig.1. Then the density of current j_r is

$$j_r = I/(\pi R^2) \quad (5)$$

According to the differential form of Ohm's law

$$j_r = \sigma\cdot E \quad (6)$$

Within the radius R, by substituting σ into Equation 4, the following can be obtained:

$$j_r E = -\frac{1}{r}d\left(\frac{r\lambda dT}{dr}\right)/dr \quad (7)$$

Assume λ is constant. Denote the temperature at r = R by T_0. Integration of Equation 7 produces

$$T = \frac{IE}{4\pi\lambda}\left(1-\frac{r^2}{R^2}\right)+T_0 \quad (8)$$

By substituting T in Equation 3, one can obtain the spectral intensity of the arc light in the column defined by $r \le R$, denoted

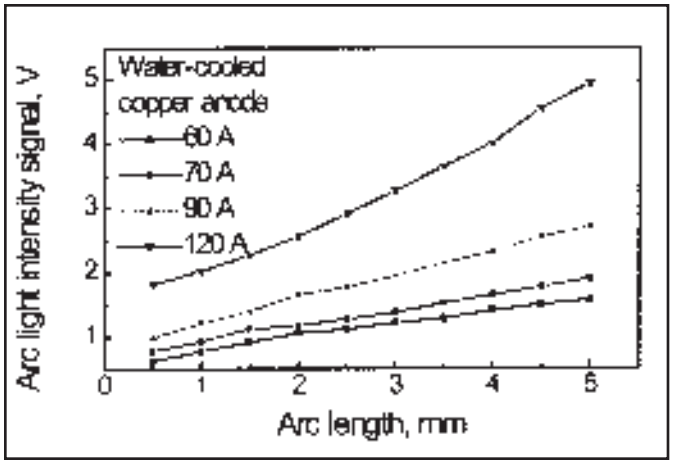

Fig. 3 — Arc light intensity vs. arc length: water-cooled copper anode.

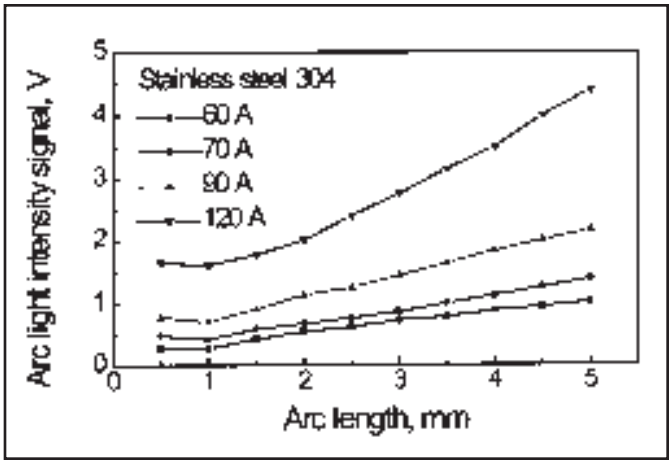

Fig. 4 — Arc light intensity vs. arc length: stainless steel anode.

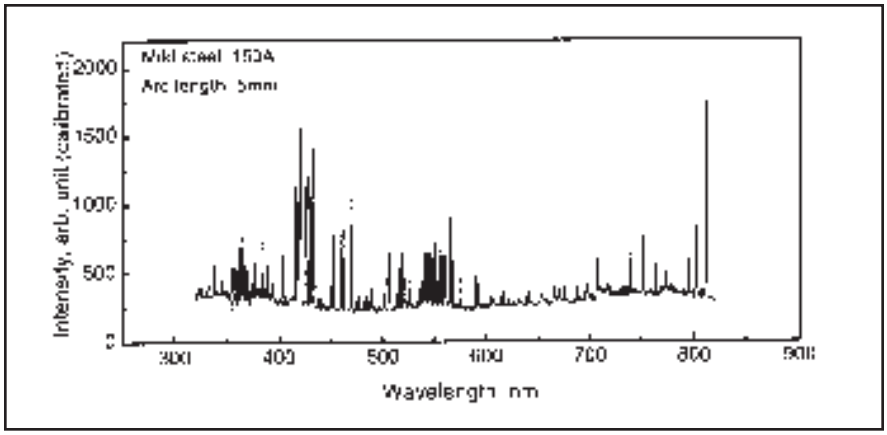

Fig. 5 — Spectral distribution of gas tungsten arc light.

by ε_{cv}, which conducts welding current

$$\varepsilon_{cv} = k'(\nu)\cdot 2k\frac{\nu^2}{c^2}\cdot\left(\frac{IE}{4\pi\lambda}\left(1-\frac{r^2}{R^2}\right)+T_0\right) \quad (9)$$

When $r > R$, $\sigma = 0$, Equation 4 becomes (Ref. 51)

$$\lambda dT = -\frac{IE}{2\pi r}dr \quad (10)$$

Its integration gives

$$T = T_0 - \frac{IE}{2\pi\lambda}\ln\frac{r}{R} \quad (11)$$

By substituting T in Equation 4, the spectral intensity of the plasma (ε_{ncv}) in the region defined by $r > R$, which does not conduct the current, can be obtained as follows:

$$\varepsilon_{ncv} = k'(\nu)\cdot 2k\frac{\nu^2}{c^2}\left(T_0 - \frac{IE}{2\pi\lambda}\ln\frac{r}{R}\right) \quad (12)$$

The arc column can be assumed to be an optical lamina, which does not absorb radiant energy. For simplicity of the derivation, the gradient of the temperature along the axis of the arc can be neglected (Ref. 51). By integrating ε_ν over the volume of arc column, one can obtain the radiant energy of the whole arc column in a unit spectral band

$$\begin{aligned} B_{i\nu} &= \iiint \varepsilon_\nu d\nu \\ &= \int_0^R 2\pi r\cdot L\cdot\varepsilon_{cv}dr + \\ &\int_R^{R_L} 2\pi r\cdot L\cdot\varepsilon_{ncv}dr \\ &= L\int_0^R 2\pi r\cdot\varepsilon_{cv}dr + \\ &\int_R^{R_L} 2\pi r\cdot\varepsilon_{ncv}dr \end{aligned} \quad (13)$$

where R_L is the radius of the arc plasma luminary and the spectral intensity of the arc plasma column is zero when $r \geq R_L$. From Equation 12, the upper limit of the integration, R_L, can be calculated as follows:

$$R_L = R\cdot e^{\frac{2\pi\lambda T_0}{IE}} \quad (14)$$

Hence,

$$B_{i\nu} = k'(\nu)\cdot\frac{k\nu^2}{c^2}\cdot L\cdot R^2\cdot\frac{IE}{2\lambda}\cdot\left(e^{\frac{4\pi\lambda T_0}{IE}}-\frac{1}{2}\right) \quad (15)$$

Equation 15 accounts for the contribution from the arc radiation. In addition to the shielding gas, other radiant sources such as the weld pool and the electrode also contribute to the observed radiation of the arc. Hence, two additional terms, I^g and constant, are added in Equation 15 to account for the contributions of heat input related sources and other sources. As a result, a modified equation is achieved as follows:

$$B_{i\nu} = k'(\nu)\cdot\frac{k\nu^2}{c^2}\cdot L\cdot\frac{I}{\pi\cdot j}\cdot\frac{IE}{2\lambda}\cdot\left(e^{\frac{4\pi\lambda T_0}{IE}}-\frac{1}{2}\right)+C_1\cdot I^g+C_2 \quad (16)$$

where j is the average current density and C_1, C_2 and g are constants. The current density remains approximately constant in the low-welding-current range and increases slowly with the welding current in the high-current range for gas tungsten arc welding (Ref. 51)

$$\begin{aligned} j &= j_c & I &\leq I^* \\ j &= j_c + a^{\,I-150} & I &> I^* \end{aligned} \quad (17)$$

where a is a small positive constant and I^* ranges from 120 to 150 A.

Equation 16 depicts the relationship between the radiation of the arc light and the welding parameters including the current, the voltage gradient of the arc column and the arc length. This comprehensive model can play a fundamental role in understanding the phenomena as-

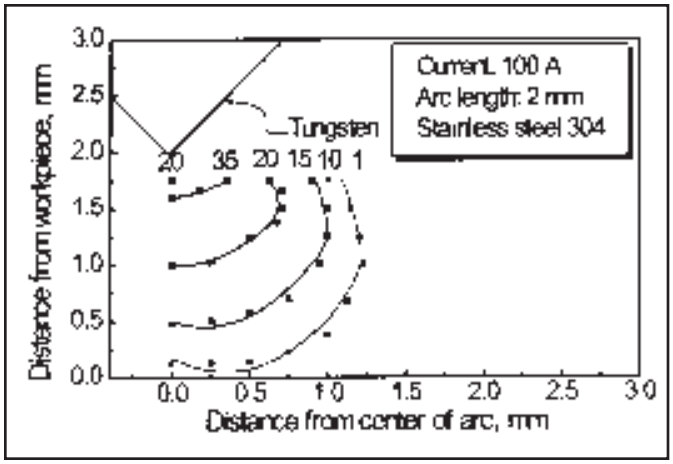

Fig. 6 — Spatial distribution of Ar atomic spectra.

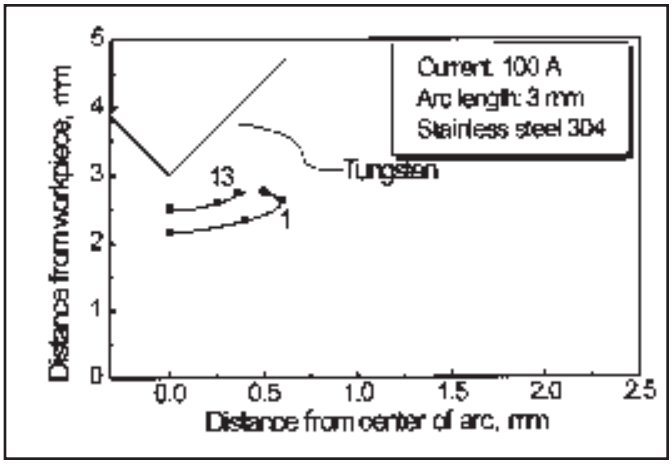

Fig. 7 — Spatial distribution of Ar ionic spectra.

sociated with arc radiation, as well as in applying the arc light sensing method to welding process sensing and control. In the following discussion, we shall first verify the effectiveness of the model through arc length sensing, and then improve the accuracy in arc length control and joint tracking based on the model.

Experimental Procedure

Experiments have been conducted toward three goals. The first one is to verify the arc light sensing model based on arc length measurement. The second has been directed to spectral analysis and improvement of arc light sensing based on arc length measurement. Finally, the arc light sensing method has been applied to joint tracking.

Water-cooled copper plate, mild steel, low-alloy steel A202M-93 and stainless steel 304 were used in the experiments. Argon was used as the shielding gas. The welding power source was an inverter welding power source with output from 5 to 500 A.

The developed arc light sensor, 15 mm in diameter and 50 mm in length, was clamped onto the welding torch. A small amount of shielding gas (0.25 L/min) passed through the sensor to cool the internal component and keep the welding smoke from the window of the sensor. The light-sensitive component of the sensor is a phototriode with spectral response from 500 to 1000 nm. An automatic sensitivity control circuit was developed to control the phototriode to make it work linearly in a large light-intensity-variation range. A grating monochrometer, with 0.1-nm resolution and 67–600 nm/min scanning speed, was used in our spectral analysis. The minimum view angle of the water-cooled probe (diaphragm) and the spectrometer is 0.015 deg, and the spectral response range of the system is 320 to 820 nm. An automatically controlled moving weld table was employed so that the welding torch and, therefore, the light path could remain stationary. The diaphragm was constructed on a three-dimensional translation stage with 0.01- mm adjustments for precise positioning. A microprocessor received the arc light signal, welding current signal, the spectral signal and wavelength signal. It also controlled the welding equipment. Data were calibrated and then transferred to a personal computer for further analysis. Figure 2 shows the overall layout of the experimental equipment. In the experiments using Layout 1, the arc light from the integral arc column or part of it was focused into the monochrometer for analysis. In partial arc spectral analysis using Layout 2, arc light from a very thin layer or a very small part of the arc column was monitored by diaphragm without peripheral effects. The data were converted by Abel transformation with the Pearce method (Ref. 46). The purpose of this experiment was to determine the spatial distribution of element emission in the arc column.

Results

Arc Length Sensing

As a primary arc welding process for precise joining of metals, GTAW requires precise control of its parameters. Arc length determines the distribution of the heat input and thus requires control as precise as 0.2 mm. Although methods such as probe, optical, arc voltage sensing, etc., have been available (Refs. 54, 55), the requirement of 0.2 mm has been difficult to realize. As will be demonstrated, arc light sensing will be a promising method to achieve such high accuracy.

Gas tungsten arc welding is relatively stable. It is reasonable to assume the radius of the electric-conducting column and the radius of the arc plasma luminary as constants. Under normal welding conditions, the voltage gradient of the arc column is also a constant. Thus, Equation 16 can be converted to

$$B_{i\nu} = G_1 L \cdot I^2 \left(e^{\frac{G_2}{I}} - \frac{1}{2} \right) + G_3 \cdot I^2 + G_4 \tag{18}$$

where G_1, G_2, G_3 and G_4 are constants, L is arc length and I is welding current. Equation 18 reveals the intensity of the arc light in a unit spectral band linearly changes with the arc length provided that the welding current remains constant.

To verify the theoretical model, several experiments have been done to measure the arc length based on arc light. Figure 3 shows the arc light signal, the integral intensity of the arc light in the band from 500 to 1000 nm, has a linear relationship with the arc length. This result was obtained on a water-cooled copper workpiece. With the least-square model fitting method, the experimental data in Fig. 3 can be described by the theoretical model with the following parameters:

$$V_{signal} = 0.0001 \cdot L \cdot I^2 \left(e^{\frac{5}{I}} - \frac{1}{2} \right) + 0.000075 \cdot I^2 + 0.0001 \tag{19}$$

where V_{signal} is arc light signal in volts. The units for the welding current I and the arc length L are ampere and millimeter, respectively.

The experimental results on stainless

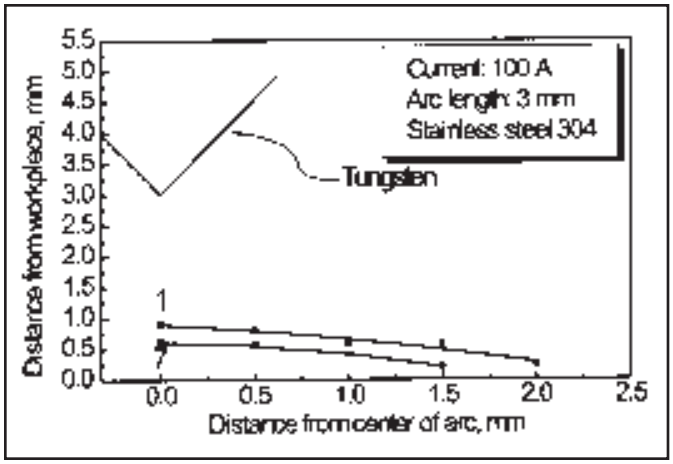

Fig. 8 — Spatial distribution of iron atomic spectra.

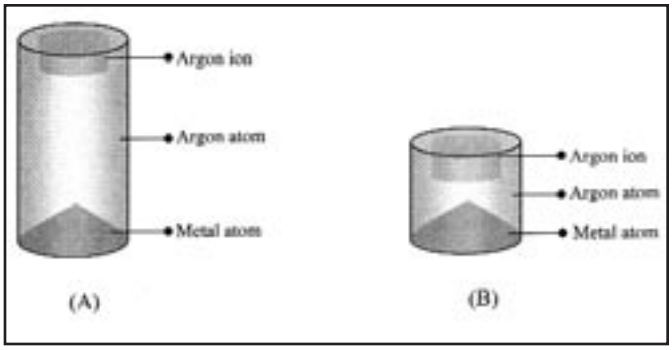

Fig. 9 — Schematic diagram of the elements and the spatial distributions of their emission intensities in the gas tungsten arc column. A — Long arc; B — short arc.

steel plates are given in Fig. 4. Although Equation 19 is in good agreement with the data when arc length is long (>1 mm), the arc light signal did not show a linear relationship when arc length decreases below 1 mm. Similar phenomena were also observed for mild steel and alloy steel. For the water-cooled copper workpiece, no melting occurred in the experiment. For other materials, melting occurred during the welding process. However, the arc length was not changed, obviously, due to the melting because very thick workpieces (>10 mm) were used in these experiments and only partial penetration welds were made. It can be deduced that some other factors caused this interesting variation in arc light signal in the short arc length range.

Improvement of Arc Light Sensing Based on Spectral Analysis

The influence of the melting phenomenon on arc light radiation implies that metal vapors play an important role when the arc length is short. Unfortunately, the melting phenomenon is an inherent feature of a practical GTAW process. Therefore, it is necessary to investigate the role of metal vapors in arc light radiation. As shown in Fig. 5, arc light emission consists of continuum and spectral lines. Besides the electrons, the emission is also corresponding to the ions and excited atoms of different elements in the arc column. In the above experiments, the arc light signal is the integration of the emissions of the continuum and lines of all the elements in the arc column. The light radiation model was derived based on the assumption the element is homogeneous in the whole arc column. It is obvious the distribution of the elements in the arc column has significant influence on the validity of the radiation model. The following investigation focuses on the spatial distribution of the major elements in the GTAW arc column.

Using the diaphragm, the spatial distribution of emission of elements in the arc column was examined. The diaphragm scanned the arc column along the horizontal and vertical direction with a step of 0.25 mm. The emission intensities of different elements were acquired with the same gain. The threshold of emission intensity was set as 1 and all absolute values were transferred to relative ones. In this way, the distribution area of different elements and their emission intensities can be compared. By connecting the geometric point with the same emission intensity, the two-dimensional emission distribution "maps" of argon atoms, argon ions and metal vapors on the cross-section plane of the arc column were produced based on Abel transformation. Because the arc column is symmetric to its axis, the cross-sectional distribution emission of elements of the arc column can reflect the situation of the whole arc column. As shown in Fig. 7, argon atomic lines are distributed throughout the arc column and account for a major portion of the radiation emitted by the welding arc. This phenomenon has been observed for different workpiece materials such as stainless steel and water-cooled copper plate, as well as for different welding currents and arc lengths. Of course, the spatial distribution of the intensity of argon atomic spectra varies, and the intensity in general increases toward the axis of the arc and the tip of the tungsten electrode — Fig. 6.

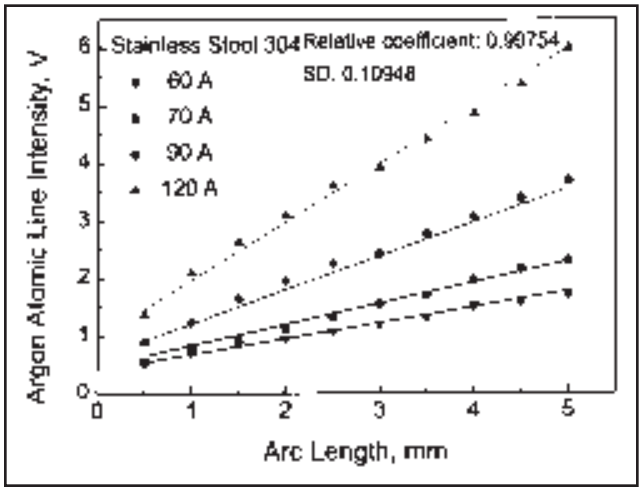

Fig. 10 — Argon atomic line intensity vs. arc length.

Different from spatial emission intensity distribution of argon atoms, the area with relatively high emission intensity of argon ionic lines concentrates immediately below the tungsten electrode, as can be seen in Fig. 7. When the distance from the tungsten increases, the intensity decreases rapidly.

The spectrum of base metal vapors is distributed in a cone concentrated just above the weld pool, as shown in Fig. 8. Its area and height have an intimate relationship with welding parameters. When the current is low, the height is large but the emission is relatively low. As the welding current increases, the height decreases and the emission of metal vapor increases. It is interesting that the metal vapor spectra are subject to severe fluctuations with random frequency. Hence, the spectral components caused by metal vapors should be filtered out to improve the accuracy of the arc length measurement.

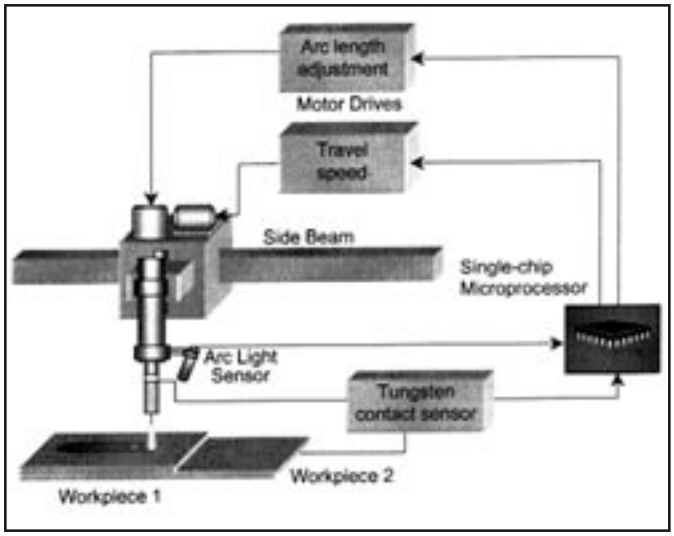

Fig. 11 — Setup of arc length control experiment.

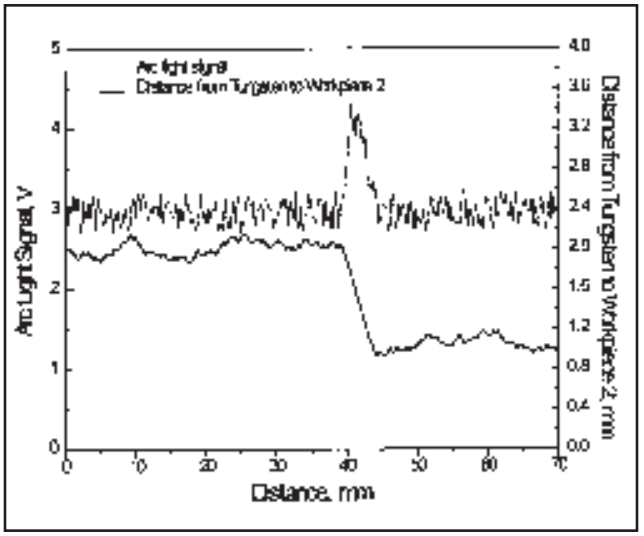

Fig. 12 — Effect of step disturbance on arc length.

It can be seen that, at the upper part of the arc column, the argon atomic and ionic lines dominate the spectrum of the arc light. The intensity of the metal lines, including the lines of vaporized tungsten and base metal, is extremely weak due to the distance from the base metal and the very high melting point of tungsten. When the distance toward the weld pool is reduced, the spectra of base metal vapor become stronger but are subject to fluctuations. As shown in Fig. 9, argon atoms, argon ions and metal atoms are distributed in a significantly different fashion in the arc column. As pointed out right after Equation 14, the equation only accounts for the contribution of the atoms of the shielding gas. The emission of argon ions and excited metal atoms do not have a direct relationship with arc length. Although we have added two terms to modify the model to account for the contributions of radiation sources other than the shielding gas, an accurate description of the fluctuated metal vapors is still difficult.

The argon atomic line is distributed throughout the arc column, independent of the workpiece material. The distribution of argon ionic lines and metal vapor lines is not even in the arc column and is prone to be influenced by other related factors, and thus cannot be used. An argon atomic line of 696.5 or 750 nm was selected based on the above experimental results. The data shown in Fig. 10 were obtained using the argon atomic line 696.5 nm. Two advantages resulted. The first is the desired linear relationship between arc length and arc light remains very well when arc length changes from 5 mm to almost short circuit, without being influenced by workpiece materials. The second is the noise in the arc light signal decreases significantly, due to the exclusion of metal vapor spectra. The relationship between experiment data of argon atomic line intensity and arc length can be regressed as

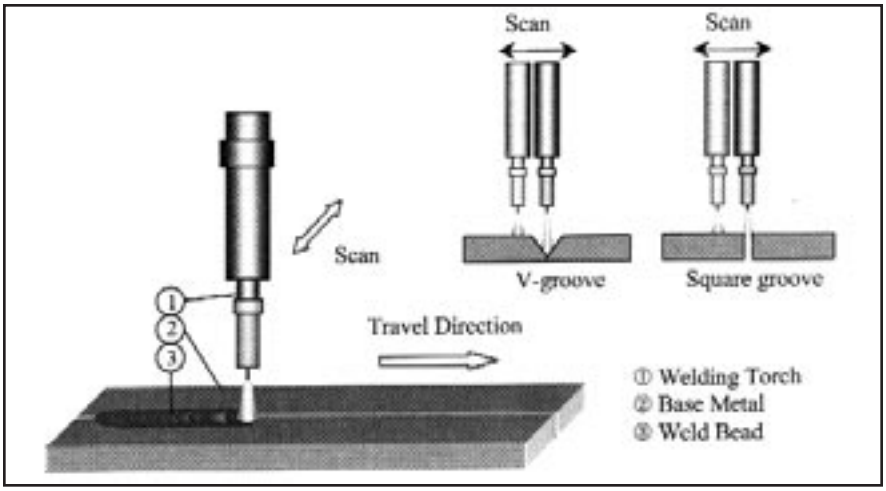

Fig. 13 — Arc light signal for detecting deviation of the welding torch.

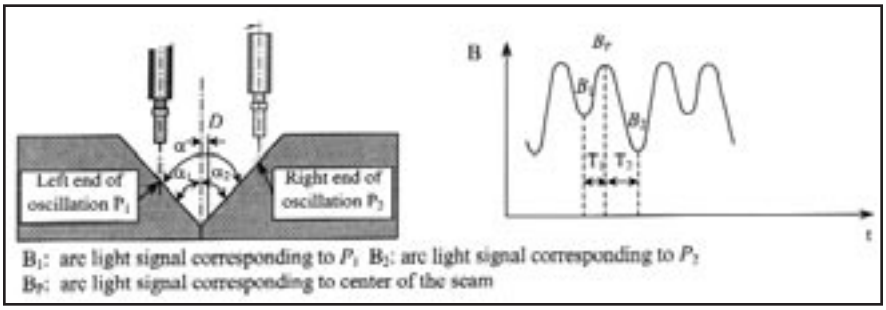

Fig. 14 — Monitoring of torch deviation based on arc light signal.

$$V_{signal} = 0.00013 \cdot L \cdot I^2 \left(e^{\frac{5}{I}} - \frac{1}{2} \right) + 0.00005 \cdot I^2 + 0.3 \quad (20)$$

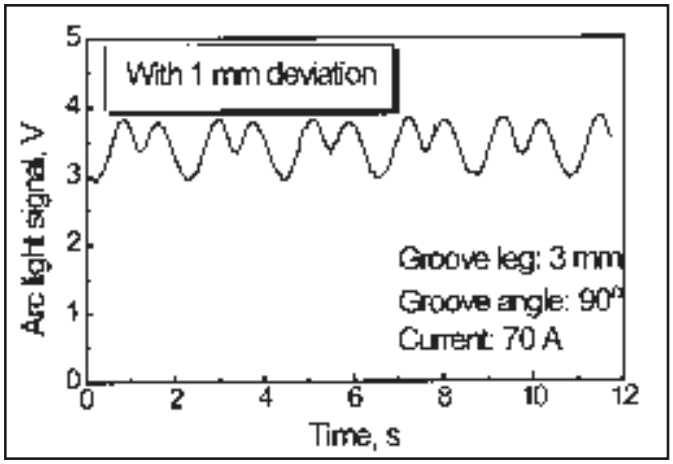

Fig. 15 — Arc light signal for detecting deviation of the welding torch.

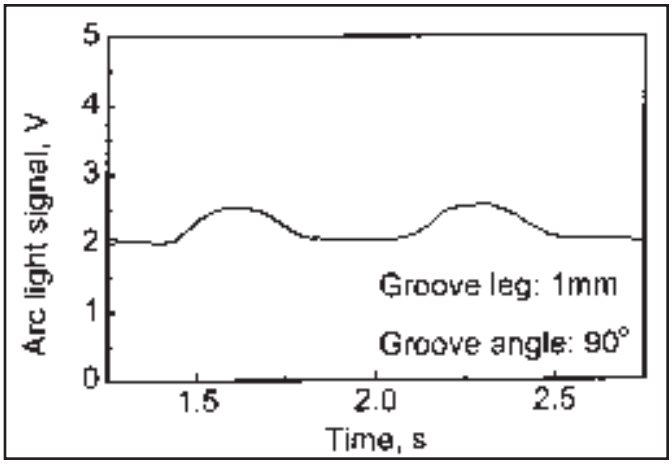

Fig. 16 — Line intensity signal in detecting small V groove.

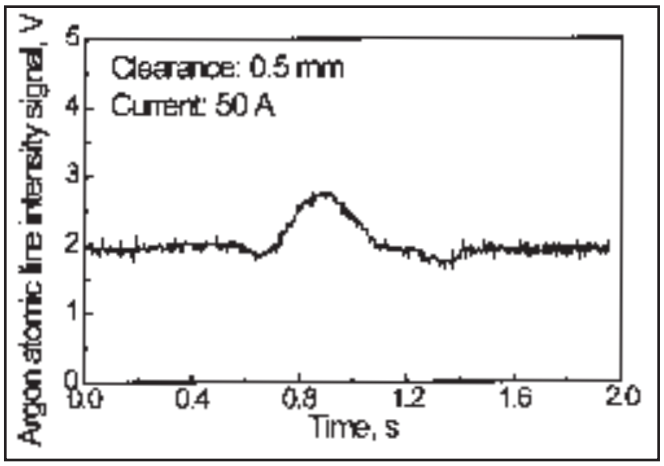

Fig. 17 — Line intensity signal in detecting a square groove in GTAW.

The dash lines in Fig.10 are the regressed results. The standard derivation is 0.1048. Equation 20 is very similar to Equation 19. Hence, the following equation has been rearranged from Equation 20 to measure the arc length in our arc length control system:

$$L = \frac{B_{signal} - N_4 - N_3 \cdot I^2}{N_1 I^2 \left(e^{\frac{N_2}{I}} - \frac{1}{2} \right)} \qquad (21)$$

where B_{signal} is the argon line intensity signal received by the arc light sensor, and N_1, N_2, N_3 and N_4 are constants. To measure and control the arc length based on Equation 21, the welding current I needs to be sampled during the welding process.

In the experiment corresponding to Fig. 12, a step disturbance in arc length was applied by overlapping a 1-mm stainless steel plate on another 1-mm stainless steel plate as shown in Fig. 11. Before igniting the arc, the torch was moved down toward workpiece 1 and a contact sensor monitored the contact between the tungsten electrode and the workpiece. When the contact was detected, the torch was moved upward for 1 mm. During welding, the single-chip, microprocessor-based control system corrected the arc length each 0.25 s based on the arc length signal using a PID algorithm. The set-point of the arc length was 1 mm and the travel speed of the torch was 4 mm/s. The arc light signal and the torch adjustment were recorded by the microprocessor. As can be seen in Fig. 12, the effect of the step disturbance on the arc length was corrected in approximately 1.5 s (6 mm travel distance). The steady-state error of the arc length was bounded by ±0.2 mm.

Weld Joint Sensing

The proposed arc light sensing method can be used to measure the weld joint and its profile for joint tracking or adaptive welding. To this end, the torch is oscillated across the weld joint as shown in Fig. 13. The weaving motion causes changes in the arc light sensed at the joint groove faces. The resultant variation in the arc light is directly proportional to the fluctuation in the distance between the surface of the weldment and the tip of the welding electrode. Fluctuations in the arc light are monitored, and the feedback signals are sent to the controller, which centers the oscillating torch in the joint. Both V-type and square grooves were used in experiments, as shown in Fig. 13.

Figure 14 illustrates the principle for detecting the deviation of the torch from the central line of the weld joint in a V groove. The deviation of the torch, denoted as D, can be determined by the following equation:

$$D = \frac{T_2 - T_1}{T_1 + T_2} \cdot \frac{L}{2} \qquad (22)$$

where L is the amplitude of oscillation, and T_1 and T_2 are the time intervals between the peak and the valleys in the waveform of the sensor output signal, as shown in Fig. 14. It can be shown that

$$\alpha_i = \arctan \left(\frac{\left(\frac{T_i}{T_1 + T_2} \cdot L \right) \cdot (B_p - B_i)}{N_1 \cdot I^2 \cdot \left(e^{\frac{N_2}{I}} - \frac{1}{2} \right)} \right) \quad i = 1,2 \qquad (23)$$

where α_i(i = 1,2) are the angles of the bevel, N_1 and N_2 are constants as defined in Equation 20, and B_p and B_i(i=1,2) are outputs of the arc light signal at the center of the joint and the end points of the oscillation, respectively. Figure 15 shows the signal when the deviation D, the leg of the groove and the included angle α are 1 mm, 3 mm and 90 deg, respectively. The difference between T_1 and T_2 indicates the deviation is clearly identifiable.

To further improve the accuracy, argon atomic lines have been used. Figure 16

depicts the atomic line signal in detecting a small V groove (1 mm). Based on the signal, the groove can be determined. Experiments showed that with argon atomic line intensity signal, 0.2 mm deviation can be reliably detected for a V-type groove with a 1-mm or larger groove leg. For butt joints, the argon atomic line signals can successfully detect square grooves when the minimum root opening is 0.5 mm for GTAW — Fig. 17. However, if an integral arc light signal is used, the minimum root opening increased to 1 mm for GTAW.

Conclusions

This study focused on the theoretical foundation for arc light sensing and its application. The major conclusions drawn from this study are the following:

1) A theoretical model of arc light radiation has been developed for the gas tungsten arc welding process. The model reveals the relationship between welding parameters, arc length and arc light intensity.

2) Spatial distributions of the emission intensities of different elements in the GTAW arc column are significantly different. The spatial emission distributions of argon ions and base metal vapors are not even in the arc column, but that of the argon atom is. By filtering out the argon ionic lines and metal atomic lines, the arc light radiation can reflect the arc length linearly and is in good agreement with the radiation model.

3) With the arc light sensing method, the arc length can be controlled within ±0.2 mm by making use of the simplified radiation model.

4) The arc light sensing has shown the effectiveness of detecting the deviation of the torch on the weld pass with a V groove and a square groove.

References

1. Horstman, S. W., Emmett, E. A., and Kreichelt, T. E. 1976. Field study of potential ultraviolet exposure from arc welding. *Welding Journal* 55(5): 121-s to 126-s.

2. Hubner, H. J., and Und, J. R. 1972. The measurement of radiation from arc welding carried out by means of various welding processes. *Welding and Cutting* 24(8): 290–293.

3. Sliney, D. H., and Freasier, B. C. 1973. Evaluation of optical radiation hazards. *Applied Optics* 12(1): 1–24.

4. Pattee, H. E., Myers, L. B., Evans, R. M., and Monroe, R. E. 1973. Effects of arc radiation and heat on welders. *Welding Journal* 52(5): 297–308.

5. Mazel, A. G., and Pumpurs, V. M. 1983. The emission properties of welding materials in arc welding. *Automatic Welding* (12): 36–37.

6. Andersen, C. B. 1986. Light emission in thermal cutting. *Welding in the World* 24(7/8): 172–176.

7. Sliney, D. H., Moss, C. E., Miller, C. G., and Stephens, J. B. 1982. Transparent welding curtains. *Welding Journal* 61(3): 17–24.

8. Haddad, G. N., and Farmer, A. J. D. 1985. Temperature measurements in gas tungsten arcs. *Welding Journal* 64(12): 339-s to 342-s.

9. Glickstein, S. S. 1976. Temperature measurements in a free burning arc. *Welding Journal* 55(8): 222-s to 229-s.

10. Shaw, C. B. 1975. Diagnostic studies of the GTAW arc (part 1—observational studies). *Welding Journal* 54(2): 33-s to 44-s.

11. Shaw, C. B. 1975. Diagnostic studies of the GTAW arc: part 2— mathematical model. *Welding Journal* 54(3): 81-s to 94-s.

12. Song, Y. L. 1995. Some phenomena and features of the component distributions in welding arc. *China Welding* 4(1): 65–69.

13. Song, Y. L. 1996. Some features of welding arc radiation. *China Welding* 5(2): 96–101.

14. Landes, K., Seeger, G., and Tiller, W. 1981. Evaluation of the mass low field and the electric current density field in a free burning TIG similar arc. *Welding and Cutting* 33(4): E14–E16.

15. Gordon, G. M., Cotter, O. A., and Parker, E. R. 1956. Effect of current and atmospheres on arc temperatures. *Welding Journal* 35(2): 109-s to 112-s.

16. Quigley, M. B. C. 1977. Physics of the Welding Arc. *Welding and Metal Fabrication* 45(10): 619–626.

17. Matsuda, F., Ushio, M., and Sadek, A. A. 1989. Gas-tungsten-electrode (report 4) — measurement of cathode temperature. *Transactions of JWRI* 18(1): 24–27.

18. Matsuda, F., Ushio, M., and Sadek, A. A. 1991. Temperature and work function measurements with different GTA electrodes. *Transactions of the Japan Welding Society* 22(1): 7–13.

19. Matsuda, F., Ushio, M., and Fujii, H. 1986. Gas-tungsten-arc electrode (report 2) — measurement of cathode temperature. *Transactions of JWRI* 15(2): 7–10.

20. Ushio, M., Fan, D., and Tanaka, M. 1993. Contribution of arc plasma radiation energy to electrodes. *Transactions of JWRI* 22(2): 201–207.

21. Kuroda, S., Fujimori, H., and Fukushima, T. 1991. Measurement of temperature and velocity of thermally sprayed particles using thermal radiation. *Transactions of the Japan Welding Society* 22(2): 10–17.

22. Kawase, R., and Kureishi, M. 1985. Fused metal temperature in arc spraying — study on arc spraying (report 3). *Transactions of the Japan Welding Society* 16(1): 82–88.

23. Shea, J. E., and Gardner, C. S. 1983. Spectroscopic measurement of hydrogen contamination in weld arc plasmas. *Journal of Applied Physics* 54(9): 4928–4938.

24. Grove, E. L., Loseke, W. A., and Gordon, E. S. 1970. Development of a portable direct reading spectrometer to monitor oxygen-hydrogen containing contaminants in gas tungsten-arc process shields. *Welding Journal*. 49(11): 538-s to 544-s.

25. Kraus, H. G. 1989. Experimental measurement of stationary SS 304, SS 316L and 8630 GTA weld pool surface temperature. *Welding Journal* 68(7): 269-s to 279-s.

26. Giedt, W. H., Tallerico L. N., and Fuerschbach, P. W. 1989. GTA welding efficiency: calorimetric and temperature field measurements. *Welding Journal* 68(1): 28-s to 32-s.

27. Kraus, H. G. 1989. Surface temperature measurements of GTA weld pools on thin-plate 304 stainless steel. *Welding Journal* 68(3): 84-s to 91-s.

28. Giedt, W. H., Wei, X.-C., and Wei, S.-R. 1984. Effect of surface convection on stationary GTA weld zone temperatures. *Welding Journal* 63(12): 376-s to 383-s.

29. Bennett, W. S., and Mills, G. S. 1974. GTA weldability studies on high manganese stainless steel. *Welding Journal* 53(12): 548-s to 553-s.

30. Mills, G. S. 1977. Analysis of high manganese stainless steel weldability problem. *Welding Journal* 56(6): 186-s to 188-s.

31. Metcalfe, J. C., and Quigley, M. B. C. 1977. Arc and pool instability in GTA welding. *Welding Journal* 56(5): 133-s to 139-s.

32. Faber, W., and Jackel, B. 1989. Practical use of an arc sensor for fillet welding. *Welding International* 3(1): 27–30.

33. Nomura, H. *An Automated Control System of Weld Bead Formation in One-Sided Submerged Arc Welding*, IIW Doc. XII-c-032-82.

34. Nomura, H.,Satoh, Y.,Tohno, K., Satoh, Y., and Kurotori, M. 1980. Arc light intensity controls current in SA welding system. *Welding and Metal Fabrication* 23(48): 457–465.

35. Salter, R. J., and Deam, R. T. 1986. A practical front face penetration control system for TIG welding. *Proceedings of International Conference on Trends in Welding Research*, pp 381–392, Gatlinburg, Tenn.

36. Connelly, C., Fetzer, G. J., Gann , R. G., and Auarand, T. E. 1986. Reliable welding of HSLA steels by square wave pulsing using an advanced sensing (EDAP) technique. *Proceedings of International Conference on Trends in Welding Research*, pp. 421–423, Gatlinburg, Tenn.

37. Deam, R. T. 1986. Weld pool frequency: a new way to define a weld procedure. *Proceedings of International Conference on Trends in Welding Research*, pp. 967–970, Gatlinburg, Tenn.

38. Johnson, *et al.*, U.S. Patent 3,236,997, Feb. 1966.

39. Wang, Q., and Zhang, L. 1992. Arc light sensing of droplet transfer in GMA welding and the real-time control of one pulse one droplet. *Proceedings of the 40th Annual Con-*

ference of the Welding Technology Institute of Australia, Vol.1, pp. 124–136.

40. Madigan, R. B., Quinn, T. P., and Siewert, T. A. 1989. Sensing droplet detachment and electrode extension for control of gas metal arc welding. *Proceedings of the 2nd International Conference on Trends in Welding Research*, pp. 999–1002, Gatlinburg, Tenn.

41. Johnson, J. A., Carlson, N. M., and Smartt, H. B. 1989. Detection of metal-transfer mode in GMAW. *Proc. 2nd International Conf. on Trends in Welding Reseach*, pp. 377–381, Gatlinburg, Tenn.

42. Chen, J. H., Fan, D., He, Z. Q.,Ye, J., and Luo, Y. C. 1989. A study of the welding mechanism for globular metal transfer from covered electrodes. *Welding Journal* 70(4): 145-s to 150-s.

43. Clark, D. E., Buhrmaster, C. L., and Smartt, H. B. 1989. Drop transfer mechanisms in GMAW. *Proc. 2nd International Conf. on Trends in Welding Research.* pp. 371–375, Gatlinburg, Tenn.

44. Wang, Q. L. 1981. The study on the relation between arc sound and arc phenomena. *Science Report of Harbin Institute of Techology* 78(9): 124–129.

45. Richardson, R. W., and Edwards, F. S. 1995. Controlling GT arc length from arc light emissions. *Proceedings of the 4th Trends in Welding Research,* Gatlinburg, Tenn.

46. Guo, Z. Y., and Zhao, W. H. 1980. *Arc and Thermal Plasma*, First Edition, Science Press (China), pp. 22–23, 260–319.

47. Song, Y. L., and Li, J. Y. 1995. Thermoequilibrium in welding arc plasma. *Transactions of China Welding Institution* 15(2): 138–145.

48. Lochte-Holtgreven, W. 1968. *Plasma Diagnostics*, John Wiley and Sons, Inc., New York, N.Y.

49. Bekefi, G. 1966. *Radiation Processes in Plasma*, John Wiley and Sons, Inc., New York, N.Y.

50. Olsen, H. N. 1957. Temperature Measurements in high current arc plasmas. *Amer. Phys. Soc. Bulletin*, p.81, January 29.

51. Kobayashi, M., and Suga, T. 1979. *A Method for the Spectral Temperature Measurement of a Welding Arc, in Arc Physics and Weld Pool Behavior,* The Welding Institute, Cambridge, U.K.

52. Cobine, J. D. 1958. *Gaseous Conductors,* McGraw-Hill Book Co., p. 290.

53. Ando, K., and Hasegawa, M. 1973. *Welding Arc Phenomena*, Sanpo Shuppan Corp.

54. Ushio, M., and Mao, W. 1994. Sensors for arc welding: adavantages and limitations. *Transactions of JWRI* 23(2): 135–141.

55. Nomura, H. 1994. *Sensors and Control Systems in Arc Welding*. First Edition, Chapman & Hall.

Preparation of Manuscripts for Submission to the *Welding Journal* Research Supplement

All authors should address themselves to the following questions when writing papers for submission to the Welding Research Supplement:

- ◆ Why was the work done?
- ◆ What was done?
- ◆ What was found?
- ◆ What is the significance of your results?
- ◆ What are your most important conclusions?

With those questions in mind, most authors can logically organize their material along the following lines, using suitable headings and subheadings to divide the paper.

1) **Abstract.** A concise summary of the major elements of the presentation, not exceeding 200 words, to help the reader decide if the information is for him or her.

2) **Introduction.** A short statement giving relevant background, purpose and scope to help orient the reader. Do not duplicate the abstract.

3) **Experimental Procedure, Materials, Equipment.**

4) **Results, Discussion.** The facts or data obtained and their evaluation.

5) **Conclusion.** An evaluation and interpretation of your results. Most often, this is what the readers remember.

6) **Acknowledgment, References and Appendix.**

Keep in mind that proper use of terms, abbreviations and symbols are important considerations in processing a manuscript for publication. For welding terminology, the *Welding Journal* adheres to ANSI/AWS A3.0-94, *Standard Welding Terms and Definitions.*

Papers submitted for consideration in the Welding Research Supplement are required to undergo Peer Review before acceptance for publication. Submit an original and one copy (double-spaced, with 1-in. margins on 8 ½ x 11-in. or A4 paper) of the manuscript. Submit the abstract only on a computer disk. The preferred format is from any Macintosh® word processor on a 3.5-in. double- or high-density disk. Other acceptable formats include ASCII text, Windows™ or DOS. A manuscript submission form should accompany the manuscript.

Tables and figures should be separate from the manuscript copy; only high-quality figures will be published. Figures should be original line art or glossy photos. Special instructions are required if figures are submitted by electronic means. To receive complete instructions and the manuscript submission form, please contact the Peer Review Coordinator, Doreen Kubish, at (305) 443-9353, ext. 275; FAX 305-443-7404; or write to the American Welding Society, 550 NW LeJeune Rd., Miami, FL 33126.